Histol Histopathol (2010) 25: 1149-1162

http://www.hh.um.es

Histology and Histopathology

Cellular and Molecular Biology

Standard bone healing stages occur during delayed bone healing, albeit with a different temporal onset and spatial distribution of callus tissues

Anja Peters[1,2], Hanna Schell[1,2], Hermann J. Bail[1,2], Marion Hannemann[1], Tanja Schumann[1], Georg N. Duda[1,2] and Jasmin Lienau[1,2]

[1]Julius Wolff Institute and Center for Musculoskeletal Surgery, Charité – Universitätsmedizin Berlin, Berlin, Germany and [2]Berlin-Brandenburg Center for Regenerative Therapies, Charité – Universitätsmedizin Berlin, Berlin, Germany

Summary. Bone healing is considered as a recapitulation of a developmental program initiated at the time of injury. This study tested the hypothesis that in delayed bone healing the regular cascade of healing events, including remodeling of woven to lamellar bone, would be similar compared to standard healing, although the temporal onset would be delayed.

A tibial osteotomy was performed in sheep and stabilized with a rotationally unstable fixator leading to delayed healing. The sheep were sacrificed at 2, 3, 6, 9 weeks and 6 months postoperatively. The temporal and spatial tissue distributions in the calluses and the bone microstructure were examined by histology.

Although histological analysis demonstrated temporal and spatial callus tissue distribution differences, delayed healing exhibited the same characteristic stages as those seen during uneventful standard healing. The delayed healing process was characterized by a prolonged presence of hematoma, a different spatial distribution of new bone and delayed and prolonged endochondral bone formation. A change in the spatial distribution of callus formation was seen by week 6 leading to bone formation and resorption of the cortical bone fragments, dependent on the degree to which the cortical bone fragments were dislocated. At 6 months, only 5 out of 8 animals showed complete bony bridging with a continuous periosteum, although lamellar bone and newly formed woven bone were present in the other 3 animals.

This study demonstrates that during delayed bone healing all stages of the healing cascade likely take place, even if bony consolidation does not occur. Furthermore, the healing outcome might be related to the periosteum's regenerative capacity leading to bony union or absence of bony bridging.

Key words: Delayed bone healing, Non-union, External fixation, Histology, Sheep

Offprint requests to: Prof. Dr.-Ing. Georg N. Duda, Julius Wolff Institute and Center for Musculoskeletal Surgery, Berlin-Brandenburg Center for Regenerative Therapies, Charité – Universitätsmedizin Berlin, Augustenburger Platz 1, D-13353 Berlin, Germany. e-mail: georg.duda@charite.de

Introduction

Bone healing is a highly complex regenerative process that recapitulates aspects of embryological skeletal development, thereby restoring injured skeletal tissue to a state of normal structure and function. This remarkable regenerative capacity may be related to the shared molecular mechanisms of fetal skeletal development and bone repair (Ferguson et al., 1998). The complex process of bone repair can be divided into five overlapping histological stages: (a) hematoma and immediate response to injury, (b) intramembranous bone formation, (c) chondrogenesis, (d) endochondral ossification, and (e) bone remodelling (Bostrom et al., 1995; Barnes et al., 1999). Numerous small and large animal models have been developed for the study of bone regeneration. These models are useful to characterize and better understand the various stages of standard bone healing and to determine how each stage can be modulated by studying e.g., the growth factors participating in the process (Barnes et al., 1999; Hadjiargyrou et al., 2002), the angiogenic process (Rhinelander, 1968), or the influence of the fixation stiffness on the repair process (Wu et al., 1984; Goodship et al., 1993; Claes et al., 1998).

Although bone repair is usually an efficient process,

delayed healing and non-unions are still severe clinical complications that can occur (Haas, 2000). There are many *in vivo* experimental models available to study delayed/non-union that have relied on biological or mechanical interventions to alter the healing process. While biological interventions such as destruction of the periosteum with or without removal of the bone marrow (Hietaniemi et al., 1995; Oni, 1995; Kokubu et al., 2003), or inhibition of angiogenesis (Hausman et al., 2001) resulted in the development of an atrophic non-union with a poor healing response, suboptimal stabilization (Hietaniemi et al., 1995; Le et al., 2001; Kaspar et al., 2004) produced a delayed healing or hypertrophic non-union with a suboptimal healing response (Megas, 2005). Most of the experimental delayed/non-union models have been used to evaluate different kinds of treatment for non-unions (Makino et al., 2005; Meinel et al., 2006) rather than to characterize and describe the biological changes that occur in atypical fracture repair. The latter approach could rationally direct the development of novel therapies.

There are only a few histological studies on the temporal onset and spatial distributions of tissue in the healing callus in such delayed/non-union models. It was shown that suboptimal stabilization does not influence the temporal and spatial characteristics of periosteal bone formation in the early phase of healing (Mark et al., 2004; Epari et al., 2006). In a rat osteotomy model stabilized with a rotationally unstable intramedullary nail, signs of undisturbed fracture healing were observed until week 3, while at a turning point of week 7, the fracture healing processes ceased (Hietaniemi et al., 1995). Volpon et al. observed two kinds of repair (atrophic or hypertrophic non-union) in a non-union model in dog that seemed to be related to the periosteal capacity of regeneration (Volpon, 1994).

To our knowledge, the histological changes that occur in mechanically induced delayed healing or non-union in large animals have not been described. Recently, we demonstrated in a sheep tibial osteotomy model that by considerably decreasing the external fixator stiffness a delayed healing, and in some cases a hypertrophic non-union, could result, as assessed by radiography and biomechanical testing (Schell et al., 2008). The aim of the present study was to histologically examine the different stages of bone healing that occur in this mechanically induced delayed healing model. Since bone healing may be considered as a recapitulation of a developmental program that is initiated at the time of bone injury, we hypothesized that the regular cascade of healing events, including remodeling of woven to lamellar bone, would be similar compared to the one occurring in standard healing (Epari et al., 2006), even though there might be differences in the temporal onset or spatial tissue distribution of the healing process that likely would not result in bony bridging. Furthermore, we expected that the different healing outcome reported at 6 months after surgery (Schell et al., 2008), in some animals delayed healing, and in others hypertrophic non-union, would be related to the periosteal capacity of regeneration leading to bony union or absence of bony bridging. To test these hypotheses, the temporal onset and spatial distributions of tissue in the healing calluses, the bone microstructure and the periosteum were examined histologically over the course of healing in sheep treated with a rotationally unstable external fixation (Schell et al., 2008).

Materials and methods

Animals

A total of 40 female merino mix sheep (2.5 years old) with a mean weight of 75 kg (± 8 kg) were randomly divided into 5 groups. All animals received a standardized mid-shaft osteotomy of the right tibia, which was stabilized with a highly rotationally unstable ("mechanically critical"), monolateral external fixator. The fixator allowed free rotation with a highly stiff stainless-steel tube set in two tapered roller bearings and was mounted on six Ø 5 mm Schanz screws (Fig. 1). Thus shear movement at the osteotomy site would be limited only by soft tissue constraints (Schell et al., 2008). Sheep were sacrificed at 2, 3, 6, 9 weeks and 6 months postoperatively (n=8, each). The 6 months time point was chosen in order to distinguish between the development of a delayed or a non-union according to the definition of a non-union in humans as a lack of radiographic evidence of union 6 months after the fracture (Ruter and Mayr, 1999; Schell et al., 2008).

All animal experiments were carried out according to the policies and principles established by the Animal Welfare Act, the NIH Guide for Care and Use of Laboratory Animals and the national animal welfare guidelines. The study was approved by the local legal representative (LAGeSo, Berlin: G0172/04).

Previously published (Lienau et al., 2005; Epari et al., 2006) histological and histomorphometrical data of the control group stabilized with a rigid external fixator (Fig. 1) leading to standard uneventful healing is presented for comparison. The control group comprised 32 female merino mix sheep (2.5 years old) with a mean weight of 64 kg (± 8 kg). These animals were sacrificed at 2, 3, 6 and 9 weeks postoperatively (n=8, each).

Surgical procedure

Under general anesthesia, the monolateral external fixator was attached medially to the non-osteotomized right tibiae by placing the Schanz screws perpendicular to the long axis of the tibia. Using a drill guide, the Schanz screws were placed in a standardized position in all animals, avoiding pre-bending between the screws. An offset distance, meaning the free length of the Schanz screws equivalent to a length of 20 mm from the skin to the fixator device, was confirmed by a spacer. A transverse osteotomy of the tibial diaphysis was performed with an oscillating saw and the bone ends

were distracted to form a 3 mm gap, ensured using a 3 mm spacer. The skin was sutured and the wound was covered with a tube bandage. After sacrifice, the tibiae were explanted for histological analysis.

Histology and Histomorphometry

Directly after harvesting (2 and 3 week time points) as well as after *in vitro* biomechanical testing (6, 9 week and 6 month time points) (Schell et al., 2008), the callus regions of the explanted tibiae were sectioned into 3 mm slices in the frontal plane. Half of the slices from each group were decalcified in EDTA, dehydrated with alcohol and xylol, embedded in paraffin and cut into 4 μm-thick histological sections. The other slices were dehydrated with alcohol and xylol and intended for calcified histology. Unfortunately, due to technical problems associated with the infiltration process during embedment, the slices from the 2-9 weeks groups and from one animal from the 6 month group were rendered unusable. Thus, only the remaining slices from the 6 months group (n=7) were embedded in methyl-metacrylate (Technovit 9100 NEU, Heraeus Kulzer, Germany), cut into 6 μm-thick sections and stained with Safranin Orange/von Kossa, which stains the mineralized tissue (black).

Paraffin-embedded sections were stained with Movat Pentachrome (Movat, 1955), which yields an excellent and colorful contrast between different tissue types such as hematoma/fibrin (red), cartilage (deep green), fibrous connective tissue (light green-blue) and bony tissue (yellow). Furthermore, cells, e.g. osteoclasts can be easily differentiated. To analyze collagen fiber orientation and thus clearly distinguish between woven and lamellar bone, sections were stained with Picrosirius Red and studied with polarization microscopy (Junqueira et al., 1978, 1979). Qualitative morphologic examination was done on Movat Pentachrome and Picrosirius Red stained sections. Previously published (Epari et al., 2006) histological data of the control group stabilized with a rigid external fixator leading to standard healing is presented for comparison.

Computerized histomorphometrical analysis was performed with an image analysis system (KS400, Zeiss, Germany) on Safranin-Orange/von Kossa stained PMMA-embedded sections of the 6 month group and on Movat Pentachrome stained paraffin-embedded sections of all groups. The region of interest (ROI) contained the osteotomy gap (gap region) and callus tissue in the proximal or distal direction, resulting in 6 mm high ROI. The width of the ROI in the medial-lateral directions was dictated by the width of the callus tissue (Fig. 2). Callus tissue composition was characterized by quantitative analysis of bone, cartilage and fibrous tissue formation. Tissue fractions [%] were calculated in relation to the callus area in the gap and periphery regions (Fig. 2). For the 6 month group, bone area fraction data from the established, more conventional analysis of PMMA-embedded sections (Lienau et al., 2005; Epari et al., 2006) was compared to that of less commonly analyzed paraffin-embedded sections to assess correlation between the two methods. Previously published (Lienau et al., 2005) histomorphometric data of the control group stabilized with the rigid external fixator leading to standard uneventful healing is presented for comparison.

Immunohistochemistry for type II collagen and alpha-smooth muscle actin

Immunohistochemistry for type II collagen was performed on paraffin-embedded sections of all groups to clearly distinguish between fibrocartilage and hyaline cartilage. Furthermore, immunohistochemistry for alpha-smooth muscle actin was performed to confirm the presence of blood vessels in the callus tissue of the 6 month group. The avidin-biotin-complex detection system (ABC method; Vector Laboratories) coupled with ALP was employed using a monoclonal anti-chicken antibody to collagen type II from mouse (Quartett, Germany) or a monoclonal anti-human antibody to alpha-smooth muscle actin from mouse (Dako, Germany), as previously described (Lienau et al., 2005). For immunohistochemistry for type II collagen, sections were pretreated with hyaluronidase and trypsin. Subsequently, qualitative morphological examination was performed on the sections.

Statistical analysis

For statistical analysis of data, medians were calculated for the different groups. Statistical comparisons between the groups were performed using the Mann-Whitney U-test for unpaired nonparametric data. For multiple pair-wise comparisons, p-values were adjusted using the Bonferroni-Holm test procedure. To compare the two histological analysis methods, the more conventional analysis of undecalcified sections and the less commonly used method of analyzing decalcified sections, the Pearson's correlation coefficient (r) was used. Furthermore, the differences between the two techniques were calculated. To accommodate the different slices and histological preparations of the osteotomy region used for both methods, the critical difference between the measured fractions of bone with the two methods was set at 10%. All statistical analyses were performed using SPSS 17.0 (SPSS Inc.). A p-value of less than 0.05 was taken as a significant difference.

Results

Qualitative histology and immunohistochemistry of the experimental group

The proximal cortical bone fragments were always dislocated in the medial direction, while distal cortical bone fragments were always dislocated in the lateral direction. The cortical dislocation extended a distance of

50-100% of the tibial diameter in both directions. Due to this dislocation, the periosteal callus width was always larger in the central, inner region of the dislocation that included both the proximal and distal inner cortical bone fragments, compared to the external, outer region (Figs. 2, 3).

At 2 weeks, intramembranous bone formation was present on the periosteal surface of all cortical bone fragments at a distance of 2 mm or more from the gap (Fig. 4A) and covered by multiple osteoblastic cells and by a broad fibrous layer of the periosteum (Fig. 5A). The periosteal woven bone in the central region of the dislocation appeared to occupy a greater area and was located closer to the osteotomy gap, compared to the periosteal woven bone at the outer region of the dislocation. The osteotomy gap was mainly composed of hematoma that also extended into the periosteal peripheral area. (Figs. 3A, 4A). Cartilage was only found in the callus of 1 out of 8 animals, appearing as a small collagen type II-positive island at the periosteal edge of the hard callus. Only a few osteoclasts were present on the cortical bone surfaces and they were completely absent in regions where hematoma remnants were found near the cortex.

At 3 weeks, the gap was filled with organizing hematoma (Fig. 3B) and fibrous tissue that appeared to be transversely aligned in all animals. In some cases, the aligned tissue was separated from each other by voids, lined by abundant cells of various shapes. Woven bone in the periosteal callus seemed to increase in area and maturity at week 3 compared to week 2 (Figs. 3B, 4B), especially in the center of the dislocated fragments, which appeared more structurally organized. In regions adjacent to the cortical bone, the bone trabeculae showed a longitudinal alignment to the tibial axis (Fig. 4B), while bone trabeculae at a distance from the cortical bone displayed a radial alignment. Additionally, the first signs of lamellar bone formation were visible near the periosteal surface of the cortical bone. Both layers of the periosteum covering the bony callus seemed to increase in thickness, especially near the gap, compared to week 2. All animals showed collagen type II-positive hyaline cartilage islands on the ossification fronts, mainly in the central region of the dislocated bone fragments. Bone formation was rarely observed endosteally and was absent intercortically, between the cortical bone ends within the osteotomy gap (Fig. 3B). Osteoclasts appeared to have increased in number in comparison to the 2 week time point, especially on the external periosteal surface of the cortical bones, adjacent to the gap.

At 6 weeks, the periosteal bony callus in the central region appeared to increase in area, while the original callus on the external periosteal surface of the highly

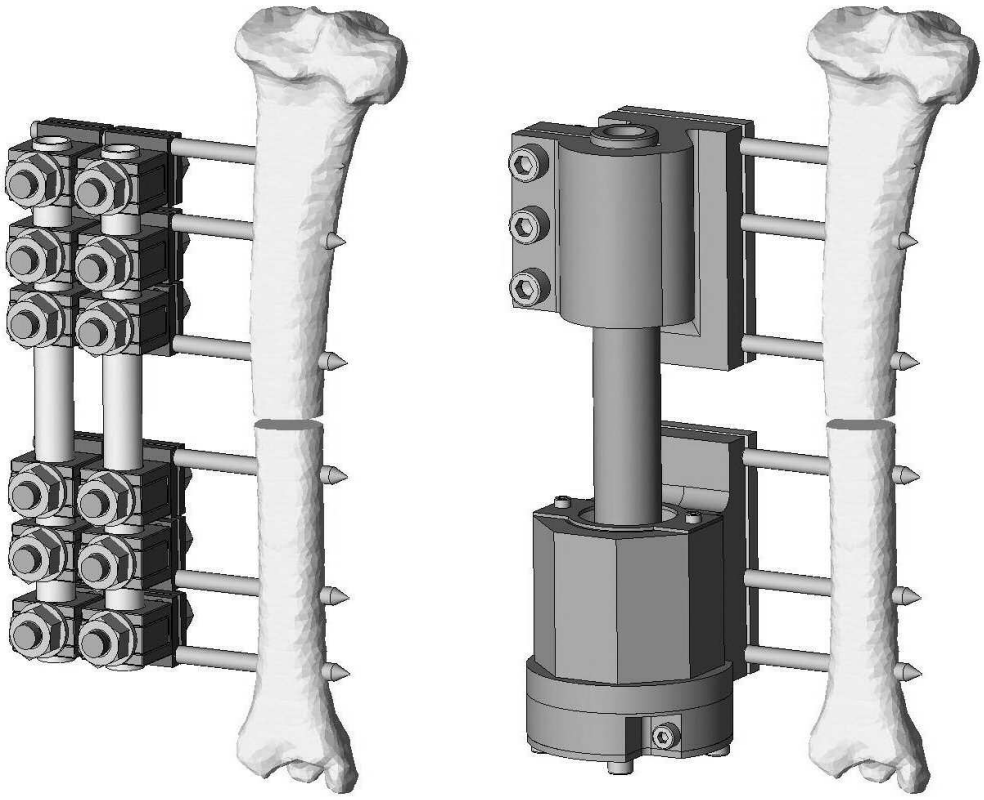

Fig. 1. Rigid (left) and rotationally unstable (right) external fixator attached to the medial aspect of the right ovine tibia (caudo-lateral view). Image modified from Schell et al., 2008.

dislocated cortical bone fragments had been mostly resorbed. The bone trabeculae appeared more compact than after 3 weeks in the periosteal region, especially adjacent to the cortical bone (Figs. 3C, 4C). In this region, lamellar bone formation had also increased in comparison to the 3 week time point. Large amounts of

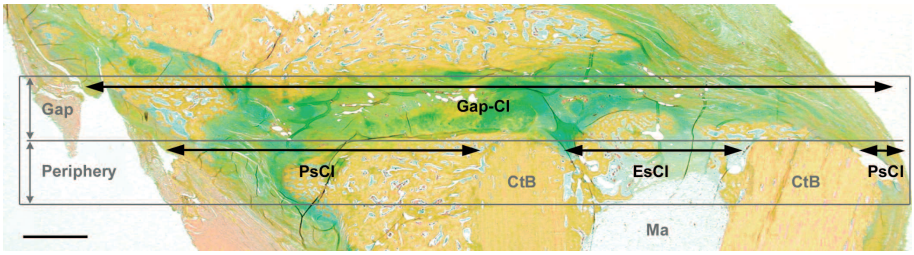

Fig. 2. Movat Pentachrome staining of an osteotomy site 9 weeks after rotationally unstable fixation. The ROI (grey box) is shown, which contained the gap (3 mm) plus the width of the gap in either the proximal or distal direction (periphery). The peripheral callus ROI was further divided into the periosteal callus (PsCl) and endosteal callus (EsCl). Due to the gross misalignment of the cortical bone fragments, the width of the periosteal callus was always larger in the central region of the dislocation than on the external, outer surface of the cortical bones. Specific regions are labeled as follows: CtB, cortical bone; Ma, bone marrow. Scale bar: 3 mm. Image modified from Lienau et al., 2009b.

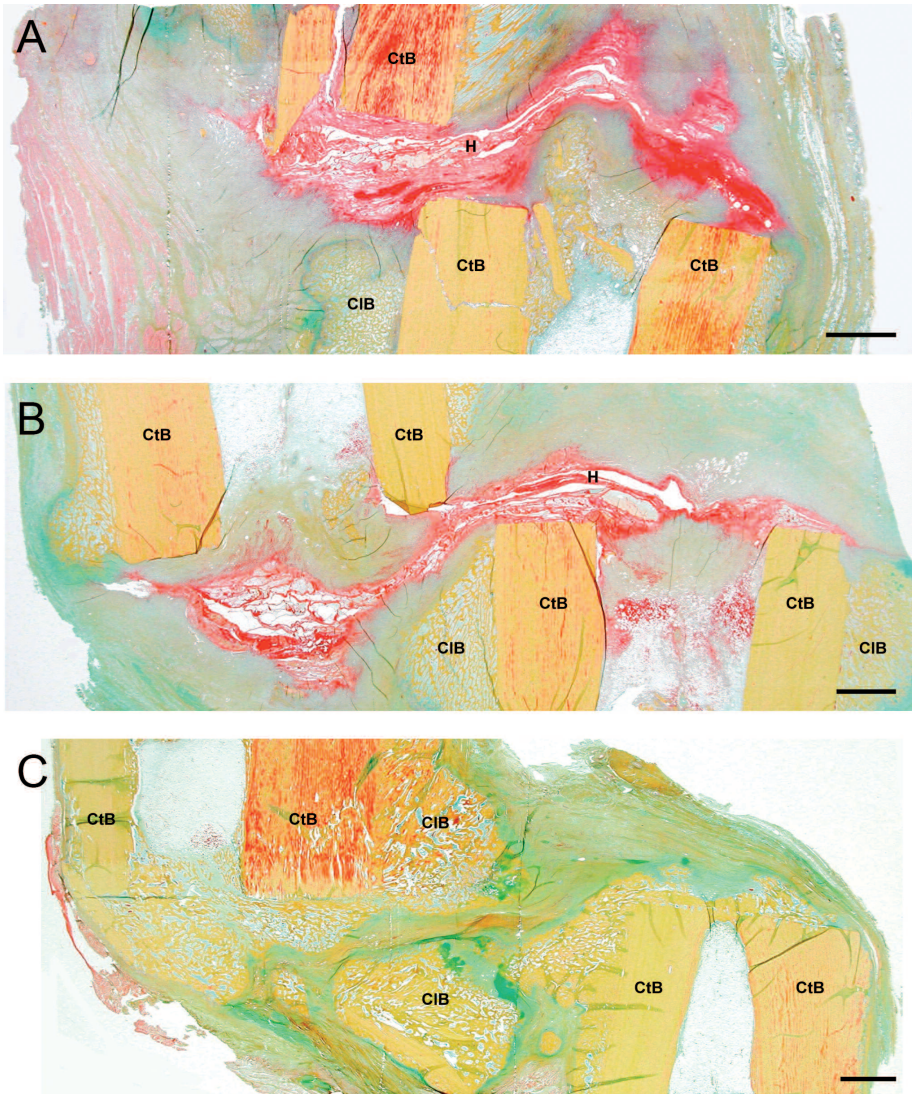

Fig. 3. Movat Pentachrome stained frontal sections through the osteotomy region 2, 3 and 6 weeks after rotationally unstable fixation. **A.** At week 2 after surgery, the osteotomy gap was mainly composed of hematoma that also extended into the periosteal peripheral area, and bone formation was present on the periosteal surface of all cortical bone fragments. **B.** At week 3 after surgery, the gap was filled with organizing hematoma and woven bone in the periosteal callus seemed to increase in area compared to week 2. **C.** At week 6 after surgery, the periosteal bony callus in the central region appeared to increase in area, while the original callus on the external periosteal surface of the highly dislocated cortical bone fragments had been mostly resorbed. The 9-week photomicrograph is shown in Figure 2. Specific regions are labeled as follows: ClB, callus bone; CtB, cortical bone; H, hematoma. Scale bars: 3 mm. Image C modified from Lienau et al., 2009a.

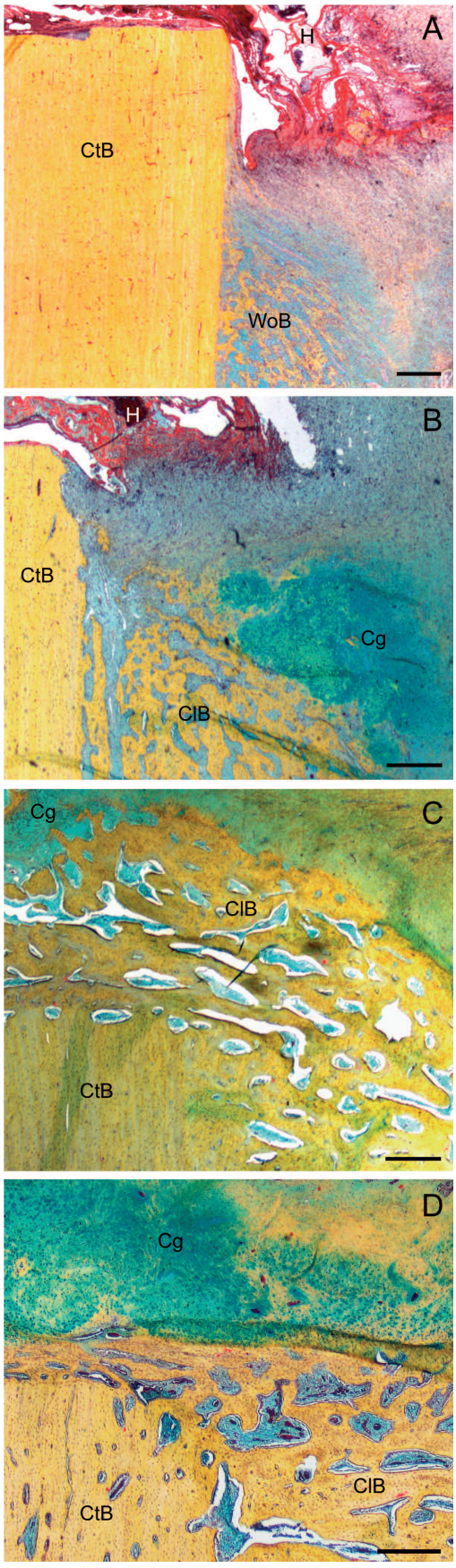

woven bone were present on the cortical bone edges narrowing the osteotomy gap (Figs. 3C, 4C). The remaining soft callus in the gap was composed of fibrous tissue and cartilage. The periosteal ossification fronts in the central region that were covered with large amounts of collagen type II-positive hyaline cartilage were not only directed towards the gap, but extended also towards the periosteal region. In three animals, varying amounts of cartilage were found in the middle of the periosteal bony callus (Fig. 5B).

In 3 out of 8 animals, bone formation was observed endosteally, while in the other 5 animals the endosteal callus was only composed of fibrous tissue and hematoma remnants. Compared to the 3 week time point, the number and size of voids that split up the transversely aligned soft tissue in the gap had increased. In 4 out of 8 animals, a large central void was present lined by one or more layers of rounded cells or by a cell-free membrane-like structure. In one instance, the central void lacked cells, containing only fluid.

The cortical bone displayed an irregular outline, appearing less compact in comparison to the 3 week time point. At 6 weeks, osteoclasts were not only found cortically, but were also visible along the surface of bone trabeculae within the osteotomy gap. Consistent with the bone resorption on the external periosteal surfaces of the cortical bone, the periosteum on these sides was thin, while in the central area of the dislocation, the fibrous layer of the periosteum had further increased in width since the 3 week time point. In 2 out of 8 animals, a continuous fibrous layer was visible on the medial or lateral side. Near the gap, the cambium layer of the periosteum was present as a broad layer of osteoblastic cells covering the ossification fronts.

At 9 weeks, no substantial change in the healing progress was seen compared to 6 weeks. Cartilage and woven bone formation continued in the central callus of the dislocated fragments, but this callus formation did not result in a bridging of the gap. Only one animal showed partial bridging of the cartilaginous periosteal callus in the center of the dislocated fragments. At this time point, woven bone formation was seen endosteally in all animals (Fig. 2). Interestingly, the external cortical bone fragments no longer displayed any bony callus.

At 9 weeks, the gap was filled with collagen type II-positive fibrocartilage and hyaline cartilage in six out of

Fig. 4. Movat Pentachrome staining of the periosteal **(A-D)** and intercortical (C, D) callus area after rotationally unstable fixation. **A.** At week 2 after surgery, woven bone (WoB) developed on the periosteal surface of the cortical bone (CtB) at a distance from the gap and the hematoma (H) extended into the periosteal area. **B.** At week 3 after surgery, hyaline cartilage (Cg) was detected on the callus bone (ClB) front and hematoma was still present. **C.** At week 6 after surgery, progression of periosteal and intercortical woven bone formation was seen. **D.** At week 9 after surgery, the osteotomy gap was mainly filled with fibrocartilage and hyaline cartilage. Scale bars: 500 μm.

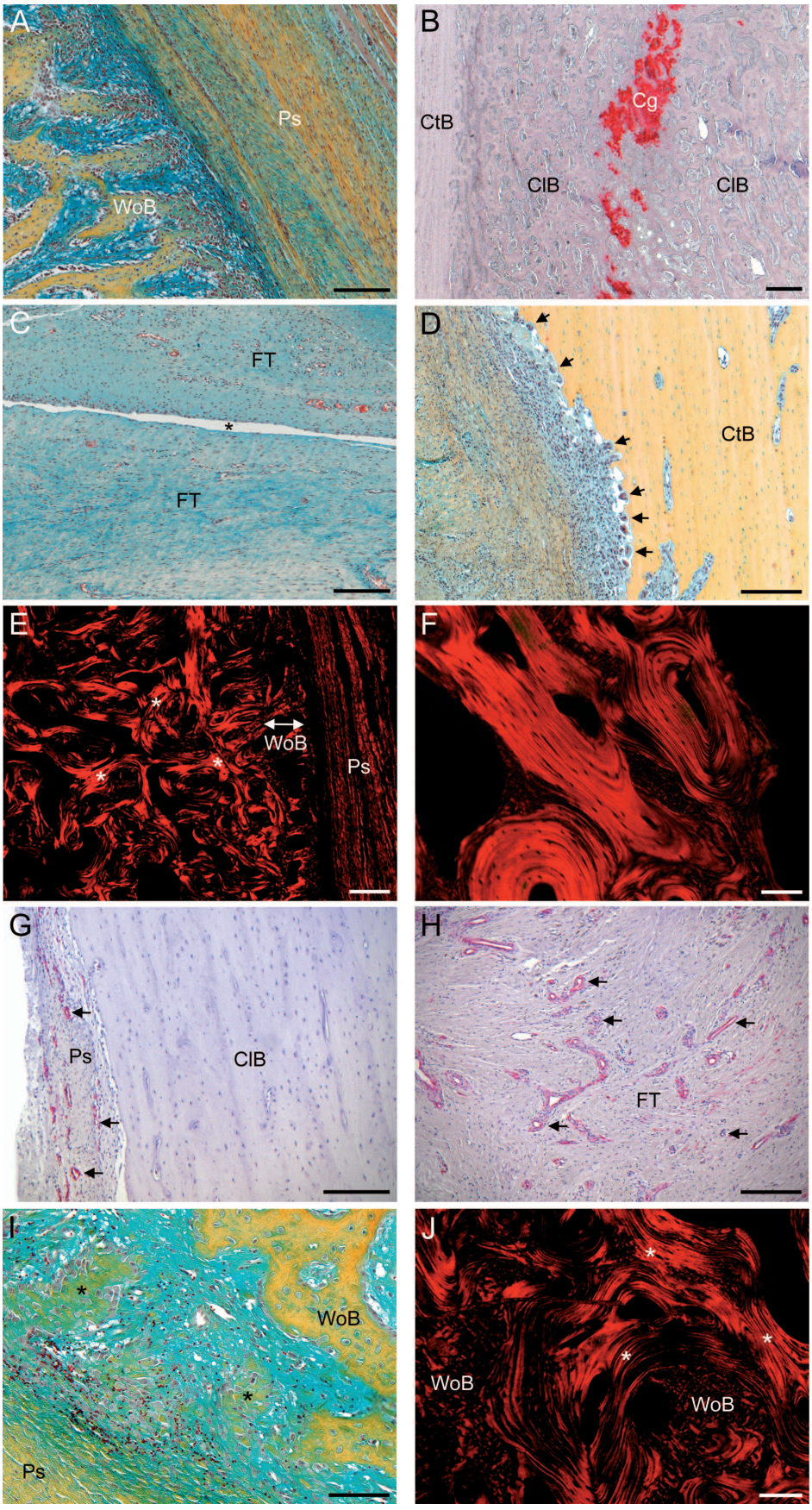

Fig. 5. Photomicrographs of representative histological sections at different time points during the course of healing. **A.** Intramembranous bone formation along the periosteum at week 2 after surgery. **B.** Periosteal cartilage formation in the middle of the bony callus at week 6 after surgery. **C.** Transversally aligned central cell-lined void (*) in the gap soft tissue at week 9 after surgery. **D.** Rows of osteoclasts (arrows) eroding the external cortical bone surface at week 9 after surgery. **E.** Periosteal bony callus composed of woven and lamellar bone (*), covered by a broadened periosteum at week 9 after surgery. **F.** Osteon-like structures with concentric lamellae at month 6 after surgery in the union subgroup. **G.** Highly vascularized (arrows) periosteum adjacent to the bridged bony callus at month 6 after surgery in the union subgroup. **H.** Highly vascularized (arrows) fibrous tissue in the central region of the fragment dislocation at month 6 after surgery in the non-union subgroup. **I.** Intramembranous bone formation (*) along the periosteum at month 6 after surgery in the non-union subgroup. **J.** Periosteal bony callus composed of woven bone and lamellar bone (*) at month 6 after surgery in the non-union subgroup. **A, C, D, I.** Movat Pentachrome staining. **E, F, J.** Picrosirius Red staining and polarization microscopy. **B.** Immunohistochemistry for type II collagen. **G, H.** Immunohistochemistry for alpha-smooth muscle actin. Specific regions are labeled as follows: Cg, cartilage; ClB, callus bone; CtB, cortical bone; FT, fibrous tissue; Ps, periosteum; WoB, woven bone. Scale bars: A, C-E, G-H, J, 200 μm; B, 500 μm; F, I, 100 μm.

eight animals (Fig. 2), but fibrous tissue and small hematoma remnants were also observed. Four out of 8 animals still showed a large central void between the tissues in the gap (Fig. 5C).

In the periosteal region, the bone trabeculae appeared more compact in comparison to the 6 week time point. Direct bone formation still continued periosteally at a distance from the cortical bone, while endochondral bone formation with opposite ossification fronts was visible towards the gap region.

The proceeding cortical remodeling was characterized by a large number of osteoclasts eroding the external cortical bone surface (Fig. 5D). Similar to the 6 week time point, osteoclasts were also present on the trabecular surface of the bony callus in the gap region. The periosteum was broadened (Fig. 5E), but still discontinuous. Only one animal showed a continuous fibrous layer of the periosteum.

The healing outcome after 6 months was quite inconsistent (Fig. 6). Five out of 8 animals showed a large bony callus of mainly lamellar bone (Fig. 5F), resulting in a complete bridging of the gap (union subgroup, Fig. 6A). However, this bridging of the cortical bone occurred along the entire width of the dislocated original cortical bone fragments (Fig. 6A). Osteoclasts were predominantly found on the external surface of the bony callus. In all animals of the union subgroup, the bony callus was completely incorporated into the adjacent cortical bone fragments in the central region of the dislocation. In most of the animals, small remnants of collagen type II positive islands were present within the bony callus. Furthermore, a highly vascularized periosteum (Fig. 5G) was visible as a continuous structure composed of a cambium and fibrous layer.

The remaining 3 animals of the 6 month group showed incomplete bony bridging of the osteotomy gap (non-union subgroup, Fig. 6B). In these animals, the gap was enlarged and contained mainly dense, highly vascularized fibrous tissue (Fig. 5H) that was transversely aligned to the tibial axis. Interestingly, no animal from the non-union subgroup showed voids between the gap tissue or hematoma remnants. The medullary cavity was partly sealed by bone, but overall the bony callus was greatly resorbed. Even so, woven and lamellar bone formation was present (Fig. 5I, J), especially on the periosteal surface of the bony callus adjacent to the gap. Only one animal showed a collagen type II-positive ossification front in the gap region and small positive cartilage remnants within the trabeculae of the bony callus. Rows of osteoclasts eroded the external cortical bone surface leading to a markedly

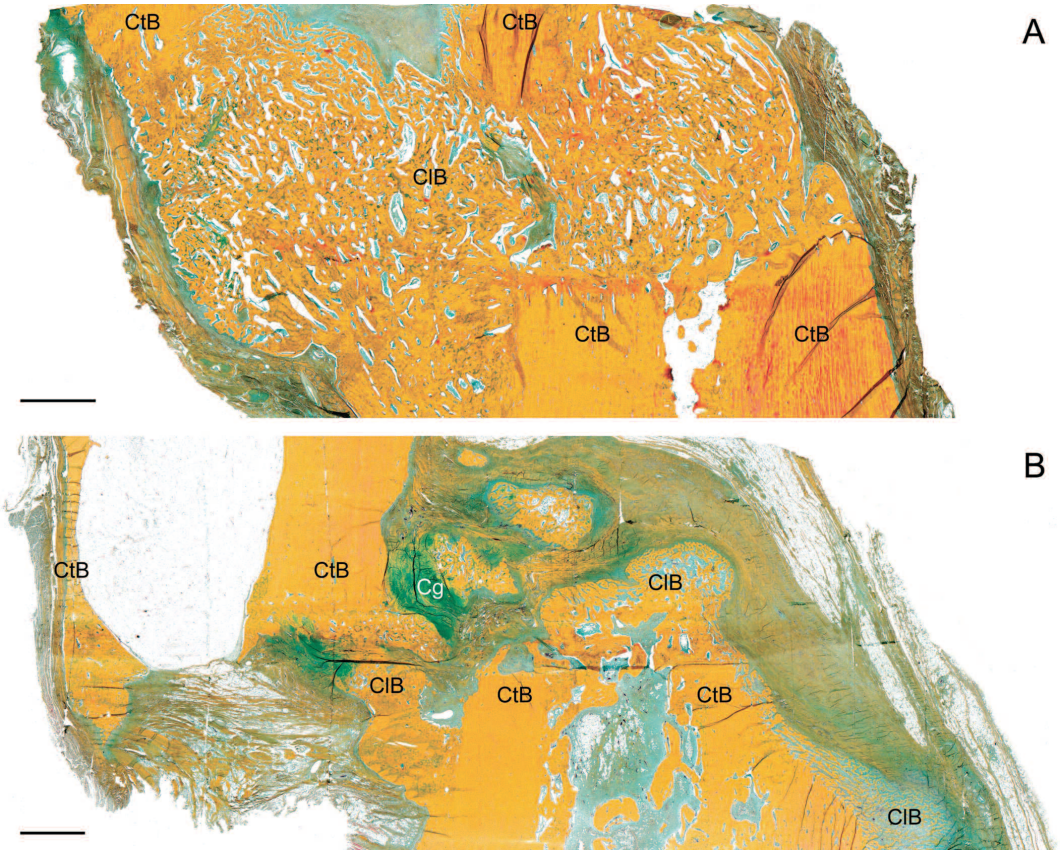

Fig. 6. Movat Pentachrome stained frontal sections through the osteotomy region 6 months after surgery demonstrating the different healing outcomes. **A.** Bony union of the dislocated cortical bone fragments. **B.** Limited bony callus formation and resorption of the highly dislocated fragment. Specific regions are labeled as follows: Cg, cartilage; ClB, callus bone; CtB, cortical bone. Scale bars: 3 mm.

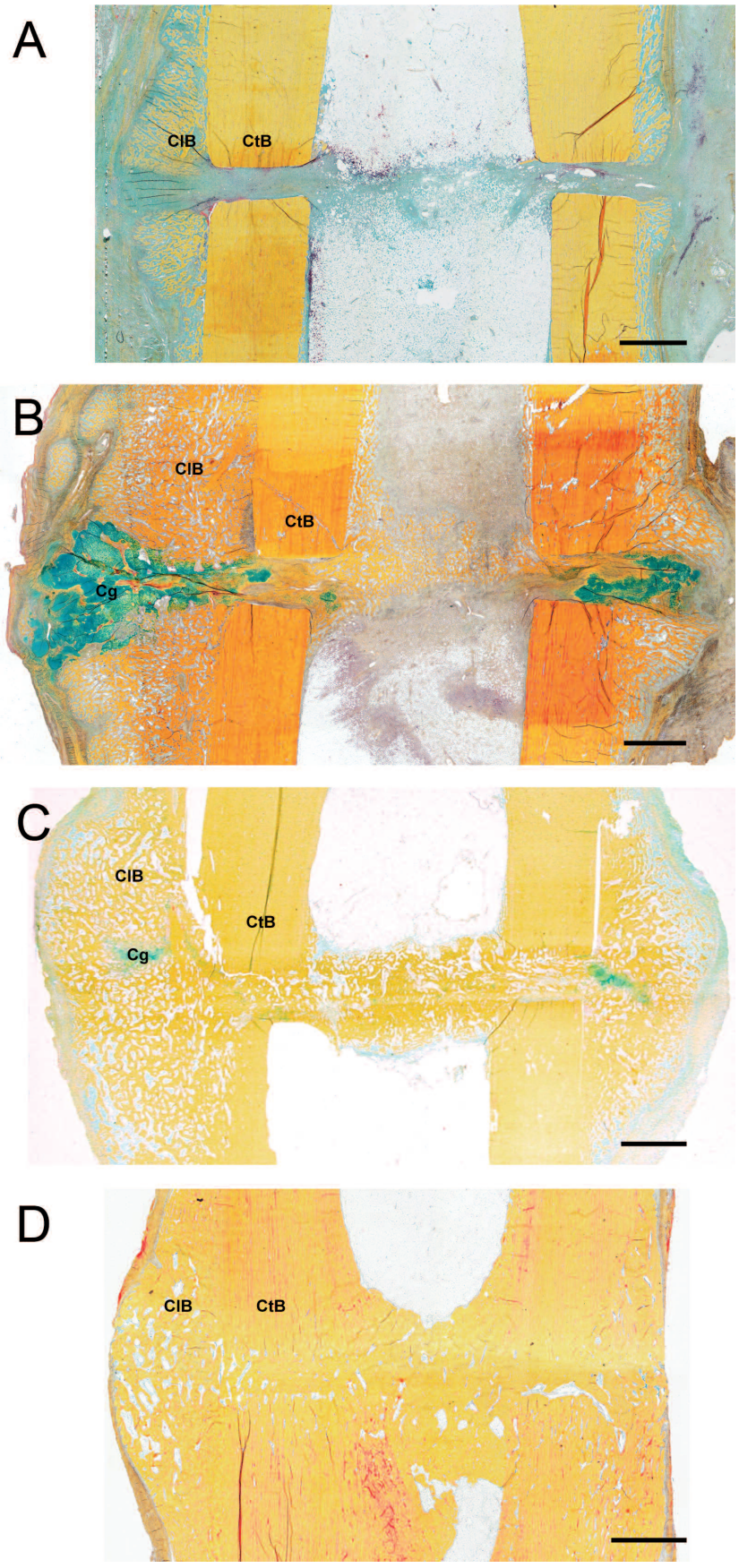

Fig. 7. Movat Pentachrome stained frontal sections through the osteotomy region 2, 3, 6 and 9 weeks after rigid fixation in the control group. **A.** At week 2 after surgery, woven bone formation was present on the periosteal cortical surfaces. **B.** At week 3 after surgery, the periosteal callus had increased in size with continued bone formation and cartilage on the leading edge of the hard callus. **C.** At week 6 after surgery, periosteal bridging with a small region of cartilage between the opposing hard callus fronts was seen. In the majority of the animals bony bridging in the endosteal and intercortial regions was also present. **D.** At week 9 after surgery, bony bridging of the intercortical zone was complete and the bony callus was completely incorporated into the adjacent cortical bone fragments. Specific regions are labelled as follows: Cg, cartilage; ClB, callus bone; CtB, cortical bone. Scale bars: 3 mm. Image C modified from Lienau et al., 2009a.

thinner cortical bone (Fig. 6B). In the periosteal regions, a highly vascularized disorganized loose fibrous tissue was found instead of a continuous cellular and fibrous layer of the periosteum.

Qualitative histology of the control group

The analysis of the control group stabilized with the rigid external fixator leading to standard bone healing was part of an earlier study and results of that group concerning the histological analysis have been published previously (Epari et al., 2006).

After 2 weeks, woven bone formation with cartilage on top was present on the periosteal, cortical surfaces and rarely observed in the endosteal or intercortical regions (Fig. 7A). The soft callus in these regions was composed of fibrous tissue. Remnants of hematoma and fibrin were only found intercortically. After 3 weeks, the periosteal callus had increased in size with continued woven bone formation in comparison to the 2 week time point. The leading edge of the hard callus was made up of cartilage (Fig. 7B). The callus bone on the cortical surface was compacted and more organized in comparison to the 2 week time point. Reorganization of

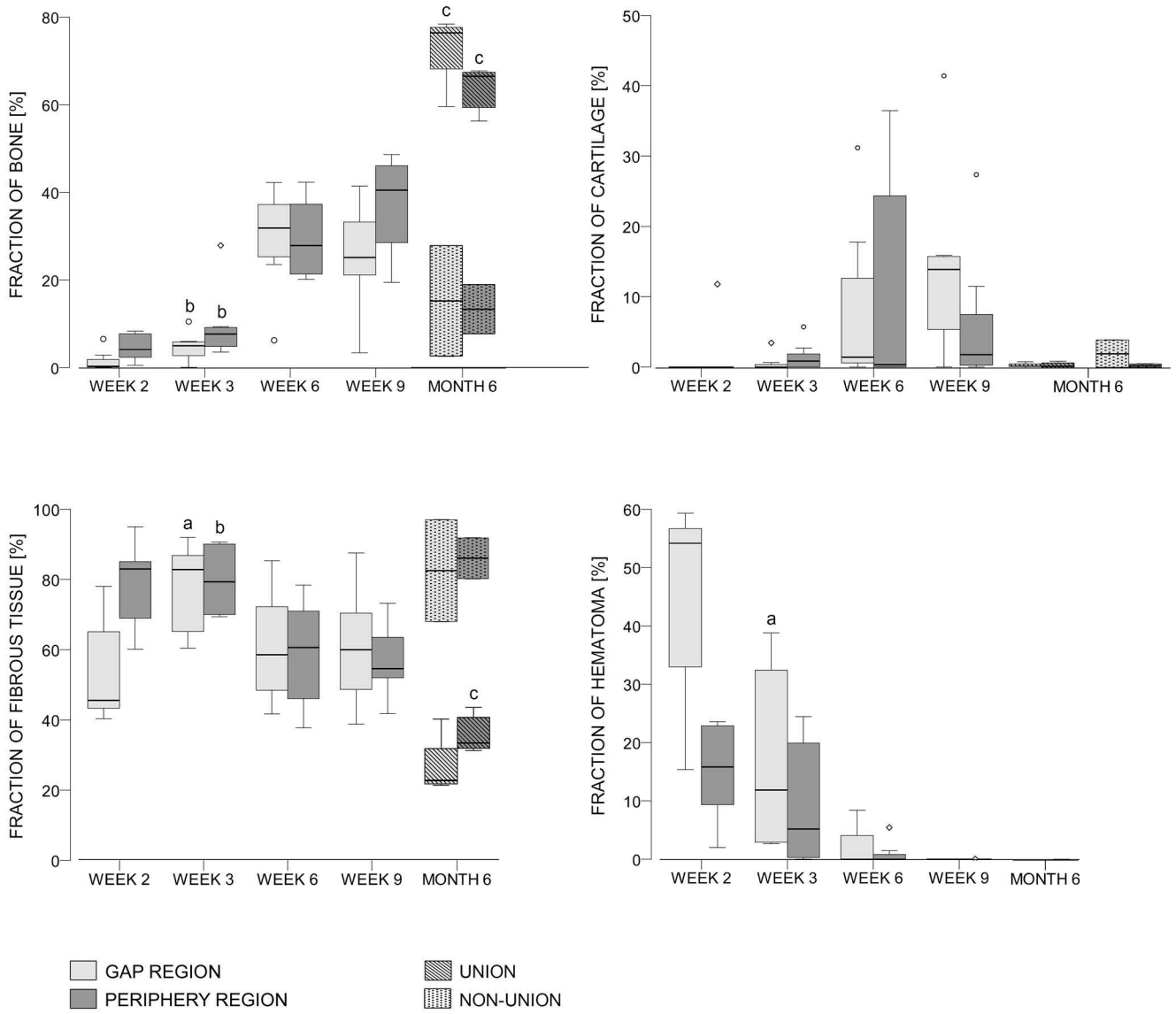

Fig. 8. Area fraction of bone, cartilage, fibrous tissue and hematoma related to the callus in the gap and periphery region over the course of healing. The 6 month group was further divided into union and non-union subgroups according to the healing outcome. [a]: p=0.005 vs. 2 week group; [b]: p≤0.01 vs. 6 week group; [c]: p≤0.012 vs. 9 week group. The circles represent statistical outliers and the diamonds represent extreme values.

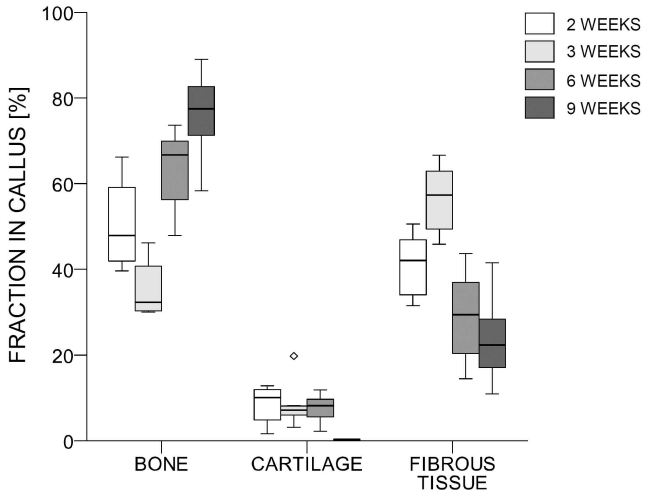

Fig. 9. Tissue fractions in the callus of the control group stabilized with the rigid external fixator leading to standard uneventful healing over the course of healing. The diamond represents an extreme value.

the periosteal woven bone into lamellar bone was seen from 3 to 9 weeks. At 6 weeks, the animals showed periosteal bridging with a small region of hyaline or fibrocartilage between the opposing hard callus fronts (Fig. 7C). Furthermore, the majority of animals showed bony bridging in the endosteal and intercortical regions (Fig. 7C). At 9 weeks, bony bridging of the intercortical zone was complete in all animals and an extensive remodeling of the cortical and callus bone was visible (Fig. 7D). The continuity of the marrow canal had been restored in the majority of the animals.

Quantitative histology (Fig. 8)

In the experimental group, the area fraction of bone in the osteotomy gap and peripheral callus region showed a temporal increase from week 2 to week 6 with significant differences measured between week 3 and week 6 (gap, $p<0.001$; periphery, $p=0.002$). In the union subgroup, there was a significant increase in the area fraction of bone in both regions from week 9 to month 6 ($p=0.002$), while in the non-union subgroup, a decrease in the area fraction of bone in both regions over this time was observed. The area fraction of cartilage in the osteotomy gap increased until week 9, but broad inter-individual variations were observed. From week 9 to month 6, there was a decrease in the area fraction of cartilage, independent of the healing outcome. The area fraction of fibrous tissue in the gap region showed a significant increase from week 2 to week 3 ($p=0.005$) followed by a decrease until week 9. In the peripheral region, the fraction of fibrous tissue remained constant from week 2 to week 3, but then significantly decreased ($p=0.01$). While in the union subgroup there was a further decrease in the fraction of fibrous tissue from week 9 to month 6, the non-union subgroup showed an increase in both regions. The fraction of hematoma in the gap and peripheral callus decreased from week 2 to week 6 with almost no detectable remnants at week 9 and month 6. In the gap region, this decrease was significant from week 2 to week 3 ($p=0.005$).

Previously published histomorphometrical analysis of the control group (Lienau et al., 2005) is shown in Figure 9 to compare with the experimental group.

Statistical comparison of the two quantitative histological methods

There was a highly significant linear correlation between the area fraction of bone in the osteotomy gap and peripheral callus region measured by the "established method with PMMA-embedded undecalcified sections" vs. the "alternative method with paraffin-embedded decalcified sections" ($r=0.995$, $p<0.001$). The median difference between both methods amounted to 3.7% ([-0.4 – 7.0]%, [Min-Max]).

Discussion

Delayed union and non-union are still challenging problems, but little is known about the biological changes that occur in atypical fracture repair. This study describes the histological changes that occur during mechanically induced delayed bone healing or non-union in sheep over 6 months of healing. We found that the normal sequence of healing events was similar, but partly delayed in comparison to that of standard healing in a sheep model, stabilized with a rigid external fixator (Epari et al., 2006), although three out of eight animals lacked bony bridging 6 months after surgery. Furthermore, we were able to show that the different healing outcome 6 months after surgery was related to the periosteal capacity of regeneration leading to bony union or absence of bony bridging.

Bone healing may be considered as a recapitulation of a developmental program that is initiated at the time of injury. Accordingly, all histological stages of bone repair (Bostrom et al., 1995; Barnes et al., 1999) were observed in the presented delayed bone healing model, although there were some differences regarding the temporal and spatial tissue distributions in the callus.

The early phase of healing was characterized by a prolonged presence of hematoma, delayed cartilage formation and a different spatial distribution of woven bone compared to a standard healing situation. The prolonged presence of hematoma in the gap may be based on a continuous rupture of existing and newly formed blood vessels in the callus (Lienau et al., 2009a) due to the large interfragmentary movements (Schell et al., 2008). Although the hematoma is considered to act as a source of signaling molecules initiating the healing cascade (Bolander, 1992), it also exhibits low levels of oxygen and glucose, as well as high levels of lactate and reductive metabolites (Street et al., 2000). This

unfavourable environment may have influenced the proliferation and differentiation of progenitor cells leading to an absence of cartilaginous or bony tissue in the periosteal region adjacent to the gap. Thus, the prolonged and extended hematoma presence may have caused the delay in cartilage formation and the different spatial distribution of woven bone at a great distance from the gap. However, the excessive interfragmentary motion may have also altered the local biochemical milieu essential for initiation of the healing cascade (Le et al., 2001; Lienau et al., 2009a,b).

It is well-known that the rate and progression of bone repair depends on the extent of interfragmentary movements (Harrison et al., 2003). Epari et al. (2006) suggest that periosteal intramembranous bone formation, at least initially, is independent of mechanical factors, whereas endochondral bone formation did appear to be influenced by the fixation stability. In concurrence, we did not observe a temporal difference in intramembranous bone formation in comparison to a standard healing situation. In contrast, the use of a rotationally unstable external fixator influenced the spatial development of woven bone unlike previous findings (Epari et al., 2006), and we did not observe periosteal woven bone formation adjacent to the gap.

Delayed cartilage formation was seen by week 3 on the hard callus fronts periosteally. Interestingly, the periosteal ossification fronts were not only advancing towards the gap, but also extended towards the periosteal region, which may be based on the dislocation and subsequent gross misalignment of the cortical bone fragments. The process of endochondral ossification did take place in our model during the 9 week healing period, but was obviously delayed due to the prolonged chondral phase, as demonstrated by large amounts of fibrous and hyaline cartilage in the osteotomy gap by week 9 with broad ossification fronts. The observed variation in cartilage formation between the animals may be based on different mechanical conditions at the osteotomy site caused by muscle forces and external loading of the limb (Schell et al., 2008).

An interesting finding was the spatial change in callus formation between the 3rd and 6th week. At week 6, cartilage and bone formation proceeded in the central region of the dislocation with remodeling of woven into lamellar bone, whereas the original callus on the external periosteal surface of the highly dislocated fragments, which was visible at week 3, had been mostly resorbed. At week 9, these cortical surfaces were lined by osteoclasts indicating further cortical resorption. The distance between the center of the callus and the external surface of the dislocated fragments appeared to be too large to enable bridging similar to critical-sized bone defects that do not bridge spontaneously (Schmitz and Hollinger, 1986).

Studies have demonstrated that although the healing outcome seems to be certain at a commonly reported time point, it is possible that the healing outcome could change at a later time point (Volpon, 1994; Hietaniemi et al., 1995). In the present study, most of the animals showed signs of a pseudarthrosis at week 9, indicated by a large central void in the gap tissue, advanced resorption of cortical bone fragments, disproportionate amounts of cartilage and limited progression of healing between week 6 and 9. Nevertheless, the long-term healing outcome remained unclear. Therefore, a later time point of 6 months was chosen according to a definition of non-unions in humans (Ruter and Mayr, 1999). By radiographic and biomechanical analyses we could already demonstrate that the healing outcome after 6 months varied between the animals (Schell et al., 2008). This different healing outcome seemed to be closely related to the periosteal capacity of regeneration, which is suggested to be crucial for complete bony consolidation (Volpon, 1994; Kokubu et al., 2003). While the non-union subgroup showed a thick fibrous layer on the periosteal callus boundary, the callus surface of the union subgroup was characterized by the presence of a complete periosteum composed of a thick, highly vascularized, outer fibrous layer and an inner layer of cells resembling bone lining cells and progenitor cells. Thus, the main difference between the two kinds of repair seemed to depend on the periosteal behavior (Volpon, 1994), but the underlying mechanism for this different regeneration capacity remains unclear.

Histological analysis of the union subgroup demonstrated the impressive capability of bone to adapt to critical mechanical conditions. After 6 months, the group showed continuous callus formation leading to a mechanically stiff union (Schell et al., 2008), even if this union also occurred between misaligned bone fragments. Due to the biomechanical conditions, caused by the large interfragmentary movements (Schell et al., 2008), resorption of the highly dislocated cortical bone fragments took place in both subgroups after 6 months, but in the union subgroup a restructuring of the tibial axis seemed to be possible. The small cortical remnant was completely incorporated into the bony callus and resorptive processes in the central callus area indicated a restoration of the medullary cavity. Histomorphometrical analysis of the 6 months group clearly demonstrated the inferior healing outcome in the non-union subgroup with a decrease in the bony fraction and an increase in the fibrous tissue fraction of the callus between week 9 and month 6. However, there was no cessation of the healing process in this subgroup. Intramembranous bone formation was still present in the central region of the dislocation and even remodeling of woven to lamellar bone was seen. Furthermore, immunohistochemical analysis demonstrated that the fibrous tissue in the gap was highly vascularized, as already demonstrated for atrophic non-unions (Brownlow et al., 2002; Reed et al., 2003). Interestingly, the non-union group lacked histological signs of instability at month 6, such as fluid-filled and cell-lined voids between tissue or hematoma remnants in the gap. Furthermore, there was a prevalence of fibrous tissue in the gap instead of fibrocartilage or hyaline cartilage resisting large

compression forces. These findings suggest that there might be other mechanisms besides callus formation that provided stability, such as muscle forces that are known to dominate the mechanical environment at the fracture site (Heller et al., 2001; Duda et al., 2003).

In general, hypertrophic non-unions are treated with rigid stabilization, since the biologic potential of the regenerative tissue is still maintained, as confirmed by our results. In our model, the mechanically-induced failure of healing was mainly attributed to a delayed and prolonged chondral phase with delayed or disturbed mineralization. Thus, in such cases, the development of a hypertrophic non-union may be prevented by rigid fracture fixation early in the healing course to address the stage of endochondral ossification.

There are some limitations to the present study design that need to be considered. The time points chosen for investigation were based on the different healing stages occurring during standard bone healing in a sheep tibia osteotomy model stabilized with a rigid external fixator (Epari et al., 2006). Since the sequence of healing events was delayed in the presented model it would have been interesting to analyze further time points between week 9 and month 6. Furthermore, the different healing outcome at month 6 theoretically requires investigation with a larger sample size. Adhering to principles associated with animal welfare and according to our initial sample size estimates, we determined that eight animals per group were sufficient. The resulting quantitative histology data at 6 months suggested an underestimation of standard deviation in our initial approximations. For technical reasons, we performed quantitative measurement of callus tissue composition on decalcified paraffin-embedded sections stained with Movat Pentachrome as an alternative method to the conventional method of examining PMMA-embedded sections stained with Safranin-Orange/von Kossa. Although the sample size for comparisons should be increased, we found a significant correlation between both methods and the difference in the fraction of bone measured by the two methods was below 10%, thus within acceptable limits.

In summary, this study describes the histological changes that occur during a mechanically induced delayed healing in a sheep osteotomy model. We found that non-union could result, despite the occurrence of all major stages of the healing cascade. Furthermore, we were able to demonstrate that the healing outcome might be related to the periosteal capacity of regeneration leading to bony union or absence of bony bridging, even under critical mechanical conditions.

Acknowledgements. This study was supported by a grant from the German Research Foundation (DFG SFB 760, Berlin) and partially by the Berlin-Brandenburg Center for Regenerative Therapies (BCRT). The authors would like to thank Mrs. Camilla Bergmann for excellent technical assistance and Dr. Bettina Willie for editing this manuscript.

References

Barnes G.L., Kostenuik P.J., Gerstenfeld L.C. and Einhorn T.A. (1999). Growth factor regulation of fracture repair. J. Bone Miner. Res. 14, 1805-1815.

Bolander M.E. (1992). Regulation of fracture repair by growth factors. Proc. Soc. Exp. Biol. Med. 200, 165-70.

Bostrom M.P., Lane J.M., Berberian W.S., Missri A.A., Tomin E., Weiland A., Doty S.B., Glaser D. and Rosen V.M. (1995). Immunolocalization and expression of bone morphogenetic proteins 2 and 4 in fracture healing. J. Orthop. Res. 13, 357-367.

Brownlow H.C., Reed A. and Simpson A.H. (2002). The vascularity of atrophic non-unions. Injury 33, 145-150.

Claes L., Heigele C.A., Neidlinger-Wilke C., Kaspar D., Seidl W., Margevicius K.J. and Augat P. (1998). Effects of mechanical factors on the fracture healing process. Clin. Orthop. Relat. Res. 355 (Supplement), S132-147.

Duda G.N., Bartmeyer B., Sporrer S., Taylor W.R., Raschke M. and Haas N.P. (2003). Does partial weight bearing unload a healing bone in external ring fixation? Langenbecks Arch. Surg. 388, 298-304.

Epari D.R., Schell H., Bail H.J. and Duda G.N. (2006). Instability prolongs the chondral phase during bone healing in sheep. Bone 38, 864-70.

Ferguson C.M., Miclau T., Hu D., Alpern E. and Helms J.A. (1998). Common molecular pathways in skeletal morphogenesis and repair. Ann. N.Y. Acad. Sci. 857, 33-42.

Goodship A.E., Watkins P.E., Rigby H.S. and Kenwright J. (1993). The role of fixator frame stiffness in the control of fracture healing. An experimental study. J. Biomech. 26, 1027-1035.

Haas N.P. (2000). Callus modulation - fiction or reality? Chirurg 71, 987-988.

Hadjiargyrou M., Lombardo F., Zhao S., Ahrens W., Joo J., Ahn H., Jurman M., White D.W. and Rubin C.T. (2002). Transcriptional profiling of bone regeneration. Insight into the molecular complexity of wound repair. J. Biol. Chem. 277, 30177-30182.

Harrison L.J., Cunningham J.L., Stromberg L. and Goodship A.E. (2003). Controlled induction of a pseudarthrosis: a study using a rodent model. J. Orthop. Trauma 17, 11-21.

Hausman M.R., Schaffler M.B. and Majeska R.J. (2001). Prevention of fracture healing in rats by an inhibitor of angiogenesis. Bone 29, 560-564.

Heller M.O., Bergmann G., Deuretzbacher G., Durselen L., Pohl M., Claes L., Haas N.P. and Duda G.N. (2001). Musculo-skeletal loading conditions at the hip during walking and stair climbing. J. Biomech. 34, 883-893.

Hietaniemi K., Peltonen J. and Paavolainen P. (1995). An experimental model for non-union in rats. Injury 26, 681-686.

Junqueira L.C., Bignolas G. and Brentani R.R. (1979). Picrosirius staining plus polarization microscopy, a specific method for collagen detection in tissue sections. Histochem. J. 11, 447-55.

Junqueira L.C., Cossermelli W. and Brentani R. (1978). Differential staining of collagens type I, II and III by Sirius Red and polarization microscopy. Arch. Histol. Jpn. 41, 267-74.

Kaspar K., Schell H., Seebeck P., Thompson M.S., Schütz M., Haas N.P. and Duda G.N. (2004). Anglestable locking of unreamed nailing reduces interfragmentary movements in a displaced osteotomy of the sheep tibia and promotes healing. J. Bone Joint Surg. (Am.) 87,

2028-2037.

Kokubu T., Hak D.J., Hazelwood S.J. and Reddi A.H. (2003). Development of an atrophic nonunion model and comparison to a closed healing fracture in rat femur. J. Orthop. Res. 21, 503-510.

Le A.X., Miclau T., Hu D. and Helms J.A. (2001). Molecular aspects of healing in stabilized and non-stabilized fractures. J. Orthop. Res. 19, 78-84.

Lienau J., Schell H., Duda G.N., Seebeck P., Muchow S. and Bail H.J. (2005). Initial vascularization and tissue differentiation are influenced by fixation stability. J. Orthop. Res. 23, 639-645.

Lienau J., Schmidt-Bleek K., Peters A., Haschke F., Duda G.N., Perka C., Bail H.J., Schutze N., Jakob F. and Schell H. (2009a). Differential regulation of blood vessel formation between standard and delayed bone healing. J. Orthop. Res. 27, 1133-1140.

Lienau J., Schmidt-Bleek K., Peters A., Weber H., Bail H.J., Duda G., Perka C. and Schell H. (2009b). Insight into the molecular pathophysiology of delayed bone healing in a sheep model. Tissue Eng. Part A 16, 191-199.

Makino T., Hak D.J., Hazelwood S.J., Curtiss S. and Reddi A.H. (2005). Prevention of atrophic nonunion development by recombinant human bone morphogenetic protein-7. J. Orthop. Res. 23, 632-638.

Mark H., Nilsson A., Nannmark U. and Rydevik B. (2004). Effects of fracture fixation stability on ossification in healing fractures. Clin. Orthop. Relat. Res. 419, 245-50.

Megas P. (2005). Classification of non-union. Injury 36 Suppl. 4, S30-37.

Meinel L., Betz O., Fajardo R., Hofmann S., Nazarian A., Cory E., Hilbe M., McCool J., Langer R., Vunjak-Novakovic G., Merkle H.P., Rechenberg B., Kaplan D.L. and Kirker-Head C. (2006). Silk based biomaterials to heal critical sized femur defects. Bone 39, 922-931.

Movat H.Z. (1955). Demonstration of all connective tissue elements in a single section; pentachrome stains. A.M.A. Arch. Pathol. 60, 289-95.

Oni O.O. (1995). A non-union model of the rabbit tibial diaphysis. Injury 26, 619-622.

Reed A.A., Joyner C.J., Isefuku S., Brownlow H.C. and Simpson A.H. (2003). Vascularity in a new model of atrophic nonunion. J. Bone Joint Surg. Br. 85, 604-610.

Rhinelander F.W. (1968). The normal microcirculation of diaphyseal cortex and its response to fracture. J. Bone Joint Surg. Am. 50, 784-800.

Ruter A. and Mayr E. (1999). Pseudarthrosis. Chirurg 70, 1239-1245.

Schell H., Thompson M.S., Bail H.J., Hoffmann J.E., Schill A., Duda G.N. and Lienau J. (2008). Mechanical induction of critically delayed bone healing in sheep: Radiological and biomechanical results. J. Biomech. 41, 3066-3072.

Schmitz J.P. and Hollinger J.O. (1986). The critical size defect as an experimental model for craniomandibulofacial nonunions. Clin. Orthop. Relat. Res. 205, 299-308.

Street J., Winter D., Wang J.H., Wakai A., McGuinness A. and Redmond H.P. (2000). Is human fracture hematoma inherently angiogenic? Clin. Orthop. Relat. Res. 378, 224-37.

Volpon J.B. (1994). Nonunion using a canine model. Arch. Orthop. Trauma Surg. 113, 312-317.

Wu J.J., Shyr H.S., Chao E.Y. and Kelly P.J. (1984). Comparison of osteotomy healing under external fixation devices with different stiffness characteristics. J. Bone Joint Surg. Am. 66, 1258-1264.

Accepted March 23, 2010